Biotribology xxx (xxxx) xxx–xxx

Contents lists available at ScienceDirect

Biotribology

journal homepage: www.elsevier.com/locate/biotri

Polymer Osmotic Pressure in Hydrogel Contact Mechanics

Kyle D. Schulze, Samuel M. Hart, Samantha L. Marshall, Christopher S. O'Bryan, Juan M. Urueña, Angela A. Pitenis, W. Gregory Sawyer, Thomas E. Angelini*

Department of Mechanical and Aerospace Engineering, University of Florida, Gainesville, FL 32611, United States

ARTICLE INFO

Keywords:
Hydrogel
Osmotic pressure
Poroelasticity
Darcy's law
Contact mechanics

ABSTRACT

Simple, semi-dilute hydrogels made from flexible polymers are often used as material surrogates for biological tissues, despite the dramatic differences between gels and tissues in their micro- and nano-structure, osmotic properties, and fluid permeability. Moreover, these simple hydrogels are often treated as poroelastic, even when applied pressures are below the hydrogel's osmotic pressure. Here we investigate the role of polymer osmotic pressure in hydrogel contact mechanics with a series of local indentation tests and bulk compression tests. Performing hydrogel indentation atop an inverted confocal microscope and applying surface pressures less than the hydrogel osmotic pressure, we find that hydrogel deformation behavior agrees with the Hertz model, observing no evidence of fluid flow or volumetric gel compression. A long-time creep of the hydrogel is also found, which can be predicted from a model of diffusive relaxations within the gel. In bulk compression tests, the gel is found to be incompressible, and therefore water cannot be driven out of the gel, unless the applied pressure exceeds the hydrogel osmotic pressure.

1. Introduction

Hydrogels have been broadly employed for many decades as material surrogates for biological tissues, largely because the elastic modulus and fluid permeability of hydrogels can be tuned to approximate the material and transport properties of various tissues [1,2]. This level of control allows the design of tribological and mechanical experiments that test fundamental questions about tissue properties while mitigating the variability within tissue samples that arise from factors such as age, sex, health of the donor, and sample preparation [2–5]. Popular hydrogel systems used as experimental tissue surrogates include polyacrylamide and polyethylene glycol, which, in their simplest formulations, are semi-dilute networks made from flexible polymers, having material and transport properties that are determined by the thermal fluctuations of their constituent polymer chains at the nano-scale [6,7]. By contrast, living tissues are complex assemblies of cells, extracellular matrix, and numerous other biopolymers and biomaterials, having material and transport properties that depend strongly on micro-scale architecture and interstitial pore space between cells [8,9]. This dominantly entropic difference between simple hydrogels and tissues may manifest in how they compress; both the elastic modulus and osmotic pressure of simple hydrogels arise from polymer thermal fluctuations and are approximately equal, while tissues behave more like bi-phasic poroelastic solids [10]. Often, the long-time dissipative response of hydrogels to compressive loads is interpreted as poroelastic without considering the role of the polymer osmotic pressure [11–13]. However, osmotic pressure of a hydrogel is a qualitatively different physical parameter from the effective compression modulus of a poroelastic solid. Thus, if the osmotic pressure dominates the hydrogel response to compressive loads, caution must be taken in interpreting the response as poroelastic and assuming pressure-driven fluid flow occurs.

Here we investigate the role of osmotic pressure in the response of a simple hydrogel system to applied, direct-contact pressure. Using a hemispherical indenter, we integrate classic contact-mechanics indentation tests with confocal microscopy, enabling the measurement of contact area, indentation depth, and applied normal load without assuming any specific elastic, viscoelastic, or poroelastic model to generate loading curves. The loading-rate dependence of hydrogel response to applied loads and evidence of fluid flow are both investigated. Applying surface pressures below the hydrogel osmotic pressure, we find that polyacrylamide gel slabs behave as described by Hertz, observing no evidence of pressure driven fluid flow. A time-dependent gel response is observed, in which the system creeps slowly under persistently applied load over very long timescales, which are hypothesized to be diffusive micro-structural relaxations within the hydrogel rather than water flow. These results are corroborated in bulk compression tests in which a thin slab is squeezed between two parallel

* Corresponding author.
E-mail address: t.e.angelini@ufl.edu (T.E. Angelini).

http://dx.doi.org/10.1016/j.biotri.2017.03.004
Received 16 November 2016; Received in revised form 4 March 2017; Accepted 6 March 2017

plates; the gel does not compress until the applied pressure exceeds the gel osmotic pressure.

2. Materials and Methods

2.1. Materials

Hydrogel samples are prepared following the methods described in Urueña et al. [7]. We prepare gels at 7.5% (w/w) polyacrylamide (pAAm) and 0.3% (w/w) bis-acrylamide crosslinker, producing networks with a mesh size of about 7 nm. 20 nm diameter red fluorescent polystyrene spheres are mixed into the polymer precursor solution before polymerization at a concentration of 0.02% (w/w) [6,7,14]. Hydrogel sheets (1 mm thick, 10 mm diameter) are cast in glass-bottom culture dishes under a glass coverslip to ensure a constant thickness for confocal imaging. After polymerization, the coverslip is removed and the hydrogel sample is allowed to equilibrate for 24 h in ultrapure water.

2.2. Indenter Configuration

In situ indentation experiments are performed with a custom microindenter as described in [15,16], mounted to a laser-scanning confocal fluorescence microscope. The custom microindenter is mounted to a piezoelectric stage that is used for vertical displacements up to 250 μm (Physik Instrumente P-622.ZCL, 1 nm resolution). The sapphire probe (1.6 mm radius of curvature) is fastened to a double-leaf flexure cantilever assembly with a normal stiffness of 40 μN/μm (~5000 μN max normal loads). Normal forces are calculated from cantilever deflections which are measured by a linear displacement capacitance probe (Lion precision C5R-0.8 sensor, 5 nm resolution). The apex of the spherical sapphire probe is centered on the microscope's optical axis for all experiments.

The system is capable of running in a load-controlled and displacement-controlled configuration, allowing the system to servo on a particular load or to follow a user defined indentation path. Reliance on a close-looped force feedback in lieu of dead weight loads allowed for other indenter characteristics such as smoothness, reflectivity, and adhesion consideration to govern material considerations over density. This design also reduced concerns with sample flatness and modulus that can be encountered in the dead load experiments.

2.3. Indentation Measurement

Prior to indentations, the sapphire probe is coated with a 0.1% (w/w) solution of F-127 Pluronic to mitigate adhesion. All experiments are performed with both the probe and the hydrogel sheet entirely submerged in ultrapure water. A normal load is chosen (500, 750, 1000, 1500, 1750, 2000, and 3000 μN) and held for a prescribed duration after which the deformed interface is imaged with the confocal microscope. Load dwell times before imaging are 0 s, 200 s, 1000 s and 3000 s. For the 1000 s and 3000 s dwell tests, the hydrogel is allowed to relax under no applied load for the same amount of time between loading steps.

2.4. Bulk Compression

The macroscopic compression test is run with a Kinexus Pro rheometer using a plate-on-plate geometry. Roughened plates are used to prevent the hydrogel from expanding radially. A 7.5% (w/w) pAAm solution is polymerized with 0.3% bisacrylamide crosslinker between the two plates (10 mm diameter) at a 0.5 mm gap. A surplus of water is placed around the plate to prevent hydrogel dehydration during the experiment. Stepped, increasing compressive loads are applied to the gel and held persistently for 90 min at each load while the change in the gap between the plates is recorded by the rheometer.

3. Results

We perform contact indentation tests on 7.5% (w/w) polyacrylamide hydrogels (pAAm) with 0.3% (w/w) bisacrylamide crosslinker (see Materials and methods). These gels are submerged in water throughout all tests reported here. Using previously published measurements of hydrogel mesh-size, we estimate the osmotic pressure to be 11 kPa using $\Pi = k_b T/\xi^3$ [7,17]. To enable visualization of the surface profile and sub-surface gel compression, we disperse red fluorescent polystyrene beads (20 nm diameter) at approximately 0.02% (w/w). To apply a controlled normal load to the gel while imaging the 3D fluorescence intensity distribution, we mount an indentation system on the bright-field illumination arm of an inverted confocal microscope, in place of the condenser lens and aperture turret. This strategy allows a 1.6 mm radius of curvature, hemispherical, sapphire indentation probe to be aligned with the optical axis. Two different indentation protocols are followed. In the first protocol, the applied normal load is ramped step-wise, holding a constant load during imaging, increasing to the next load, holding, imaging, and so on. In the second protocol, the normal load is completely removed between increasing steps, providing long times for potential hydrogel relaxation and recovery.

In the step-wise ramping measurements, normal loads are held at 500 μN, 750 μN, 1000 μN, 1500 μN, 1750 μN, 2000 μN, and 3000 μN (Fig. 1 A). The ramping rate between normal load steps is 200 μN/s, and before imaging the load is held for 200 s before confocal z-stacks are collected. Each confocal stack takes 100 s to collect. The z-stacks are azimuthally averaged around the vertical axis of symmetry centered on the apex of the indenter (Fig. 1 B). The resulting R-Z intensity profiles are thresholded to determine the indented gel surface profile (Fig. 1 C), and the edge of contact is identified by finding the location where the gel surface diverges from the known indenter shape (Fig. 1 D). The contact width, a, at each load can be converted into an indentation depth, d, producing a force-indentation curve. The normal load scales like $d^{3/2}$ as predicted by the Hertz model, which we fit to the data to determine the hydrogel composite modulus, finding $E^* = 26$ kPa (Fig. 2).

To explore the potential role of rate-dependent dissipation and stress relaxation that may arise from poroelastic effects, we perform a series of indents in which the gel is allowed to recover between static normal loads by fully retracting the indenter. Here, each load is treated as an individual indentation, held for a chosen time, and imaged. After imaging, the hydrogel is allowed to equilibrate under no load before increasing the load for an equivalent time period. Two separate 7.5% pAAm hydrogels samples are used, loaded and unloaded for both 1000 s and 3000 s. For the 1000 s experiment, a measurement is also taken immediately after the target load is reached, creating another dataset with a 0 s delay under load. Performing the same analysis as described above, we find Hertz scaling for all three tests, and E^* of 32 kPa, 26 kPa, and 35 kPa for the 0 s, 1000 s, and 3000 s protocols. The lack of a systematic trend in these data and their overlap with the progressive load data suggest that negligible time-dependent behaviors contribute to the mechanical response of hydrogels to contact forces.

Given the agreement between our data and the Hertz contact model, we use the Hertz model to determine the maximum applied pressure across all the tests, at the apex of the indenter. This predicted maximum pressure is 6 kPa, which is significantly less than the 11 kPa osmotic pressure of the hydrogel, suggesting that the gel is maintaining a uniform polymer concentration throughout the indentation process and preventing fluid flow. The 3D confocal images are used to observe whether polymer is concentrating below the indenter; if the hydrogel is concentrating near the surface, the voxel intensity should increase with applied load. Thus, we measure the fluorescence intensity at all discrete loads near the surface at a radial distance of 100 μm from the center. No correlation between the indentation depth and fluorescence intensity is found, confirming that during the indentation process the gel is not concentrating.

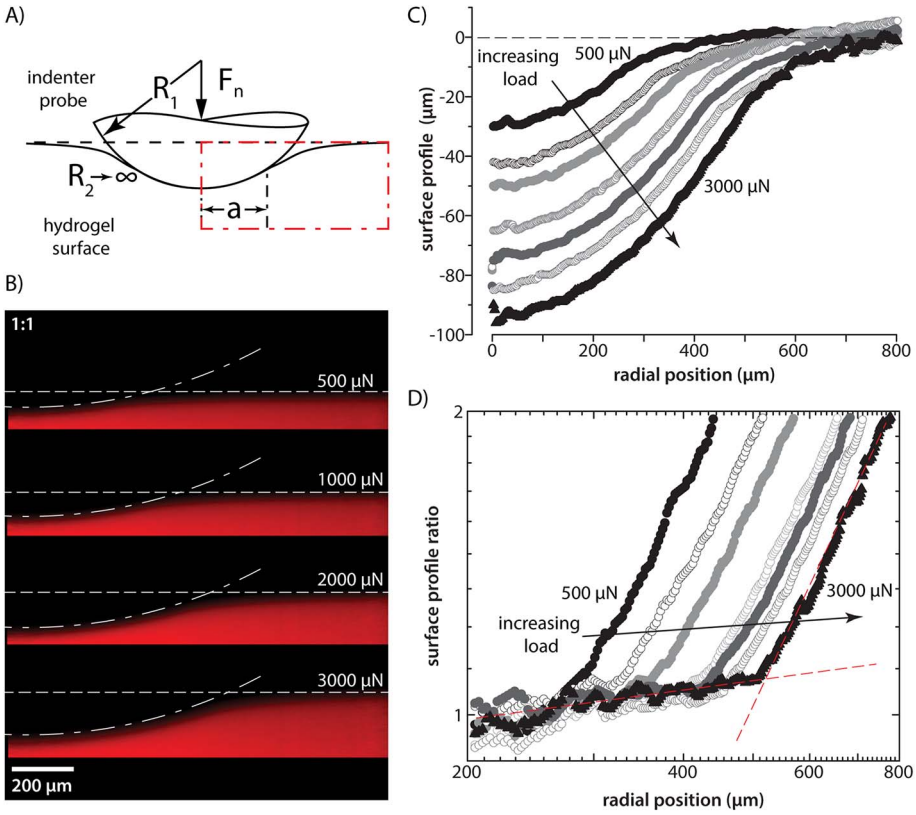

Fig. 1. Hydrogel indentation with a rigid spherical probe on a confocal microscope. (A) A schematic of a hemispherical probe of radius R_1 indenting an elastic half-space with a normal force, F_n. The red region of interest shows the contact half width, a (B) Azimuthal average of the confocal stack, showing the deformation of the hydrogel surface at normal loads of 500, 1000, 2000, 3000 µN. The un-deformed surface is noted by the horizontal dashed line, and the profile of the sapphire probe is represented by the dotted-and-dashed line. (C) Indented surface profiles for normal forces of 500 µN, 750 µN, 1000 µN, 1500 µN, 1750 µN, 2000 µN, and 3000 µN. (D) A surface profile ratio is computed by dividing the known hemispherical indenter profile by the indented gel surface profile. The edge of contact is determined from the point where the profile ratio rapidly rises. (For interpretation of the references to colour in this figure legend, the reader is referred to the web version of this article.)

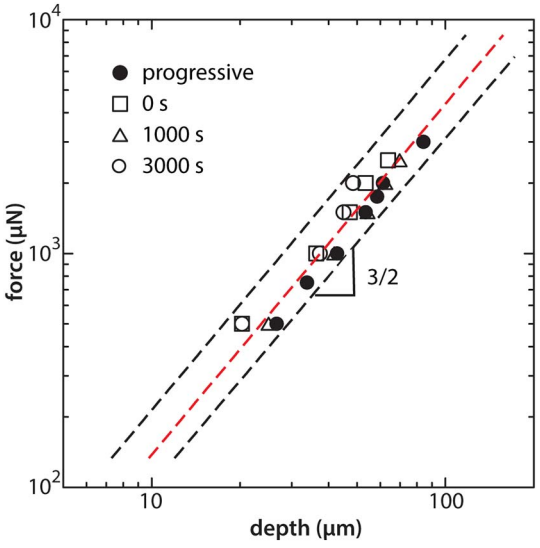

Fig. 2. Normal force vs. indentation depth for each experiment. The force increases with indentation depth to the 3/2 power. Using Hertz' contact theory, the elastic modulus averaged over all experiments is $E^* = 29$ kPa. The dashed red line represents the fit through all data sets with the dashed black lines bound all sets. (For interpretation of the references to colour in this figure legend, the reader is referred to the web version of this article.)

If no fluid flows under these modest levels of applied pressure, then the volume displaced by the indenter must be accounted for because water is incompressible at these pressures. The hydrogel tested here is confined on all sides except for the top surface, so the indented gel must bulge upward, outside of the contact area. The gels indented here are approximately 1 mm thick and 2 cm in diameter, with a corresponding volume of 314 mm^3. At the maximum apex indentation depth of 100 µm, using a 1.6 mm radius indenter, the volume that must be accounted for is 0.05 mm^3, or 0.016% of the total gel volume. Assuming a uniform upward bulging the gel outside of contact, the potential rise of the gel surface location in the far field is 160 nm, which is far beyond the optical sectioning capability of the low-magnification, long-working distance objective that is used with the method described here. Accordingly, no upward bulging in the immediate vicinity of the indenter is observed; further experimentation measuring the gel surface in the far-field must be performed to measure this potential effect.

To test the potential role of osmotic pressure in hydrogel compression with an independent experiment, macroscopic compression tests are performed by casting a hydrogel disc between roughened parallel plates in a rheometer. Sequentially increasing loads are stepped through, in which a constant load is applied to the hydrogel for 90 min between steps and the amount of hydrogel compression is measured. Below an applied pressure, P, of 10 kPa, the hydrogel supports the load with no apparent change in hydrogel thickness, δ_H. At applied $P > 10$ kPa, the hydrogel thickness decreases linearly with pressure (Fig. 3). The hydrogel is cast as a thin slab with a thickness of 0.5 mm and diameter of 20 mm and does not expand radially during these tests. As the hydrogel compresses, the polymer concentration is therefore proportional to the thickness of the slab. The linear relationship between compression and applied pressure for $P > \Pi$ is consistent with an ideal gas equation of state for this simple hydrogel. The small amount of compression observed at $P < \Pi$ may arise from the roughness of the parallel plates, which is measured with scanning white light interferometry. An average roughness of 5 µm on each of the two plates

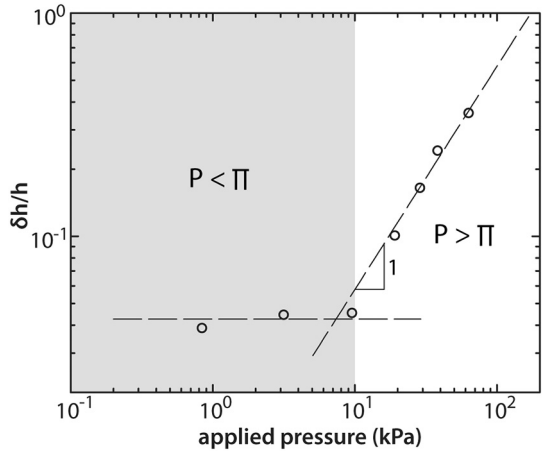

Fig. 3. Results of compression experiments performed with a flat hydrogel sheet between parallel plates. The hydrogel is insensitive to increasing applied pressure up to 10 kPa after which the hydrogel compresses linearly with increasing applied pressure. This threshold pressure is approximately the hydrogel osmotic pressure, which we estimate to be 11 kPa.

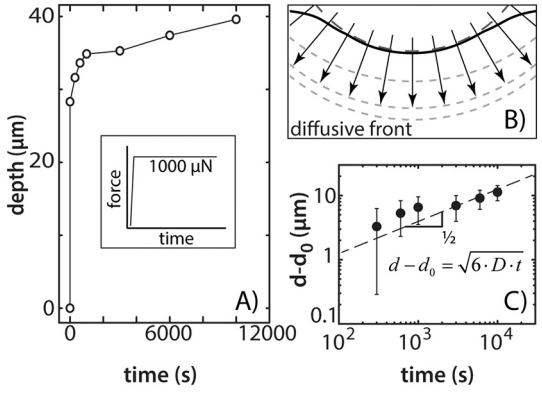

Fig. 4. Long-time relaxation of a 7.5% pAAm gel under local contact pressure. (A) Indentation depth versus time during a persistent 1000 μN load held for 10,000 s. (Inset) Step-loading profile for the persistent test. The steady force was reached in approximately 5 s after contacting the hydrogel surface. (B) The hemispherical indenter moves like a classical diffusing front. (C) After the immediate elastic indent to depth d_0, the hemisphere continues to deform the gel, increasing in depth with time to the ½ power, consistent with diffusive dynamics. Uncertainty intervals are estimated from the envelope of variation defined by all experiments shown in Fig. 2.

is found.

At applied pressures less than the polymer osmotic pressure, we have not observed evidence of increased polymer concentration accompanied by water flow. However, it is possible that long time-scale structural relaxations occur in the gel that do not involve water flow. It is well known that equilibrium heterogeneities in polymer concentration occur spontaneously in polyacrylamide hydrogels, and have a characteristic length-scale of about $R = 1$ μm [18,19]. These micro-heterogeneities can be thought of as spatial variations in polymer concentration with a characteristic wavelength of R, which fluctuate as small collectives, driven by thermal forces. Using the Stokes-Einstein equation, $D \approx k_B T/(6\pi\eta R)$, a diffusion coefficient for these micro-scale domains can be estimated. Here, k_B is Boltzmann's constant, T is the temperature, and η is the solvent viscosity. For a strongly solvated polymer like polyacrylamide, we use the effective viscosity of bound water, approximately equal to 0.1 Pa s [20]. The resulting diffusion coefficient is $D = 2 \times 10^{-15}\,\mathrm{m^2\,s^{-1}}$.

One way to view this prediction is that it would take about 10^4 s to drive an indenter into a hydrogel by 10 μm if the time-scale is controlled by spontaneous diffusive fluctuations of micro-heterogeneities, rather than by pressure driven flow. To explore this prediction, a long-time indentation experiment is performed with the microscope-mounted indentation system, described above. A 1000 μN load is applied to a hydrogel sheet and held statically for 10,000 s. During this hold, confocal stacks are acquired at discrete time-points. A large, immediate indent is observed, followed by a very slowly rising indent over the remaining 10^4 s (Fig. 4 A). Treating the immediate deformation as purely elastic, indenting to a depth d_0, we follow the remaining increase over time, $d(t) - d_0$. Plotted on a log-log scale, $d(t) - d_0$ rises with time to the ½ power, characteristic of diffusion (Fig. 4 B,C). Fitting a simple diffusion power law to these data, given by $d(t) - d_0 = (6Dt)^{1/2}$, a diffusion coefficient of $D = 1.7 \times 10^{-15}\,\mathrm{m^2\,s^{-1}}$ is found, in excellent agreement with our prediction. Thus, long time-scale, transient indentation responses in hydrogels may occur even when the applied pressure is below the polymer osmotic pressure where polymer concentration is unlikely to change and fluid flow is unlikely to occur.

4. Discussion

The osmotic pressure of a fully swollen, semi-dilute hydrogel made from flexible polymers can be thought of in analogy to a compressed gas. If one considers a pressure vessel with a movable piston at one end, filled with a pressurized gas, it is obvious that the piston cannot be displaced inward unless an external pressure that exceeds the internal gas pressure is applied to the outside of the piston. The parallel phenomenon occurs with polymer solutions inside of dialysis bags. A water-permeable dialysis bag, filled with a semi-dilute polymer solution, will swell to equilibrium when placed in a good solvent (water, in our case). If polymers are added to the external bathing solution, the dialysis bag will not compress until the osmotic pressure of the external polymer solution exceeds the osmotic pressure of the internal polymer solution – much like the pressurized gas vessel behaves. One can further imagine adding sufficient polymer to the external bathing solution to just balance the osmotic pressure without compressing the bag, then adding crosslinks to the semi-dilute polymer solution inside of the bag. If just the right amount of crosslinker is added to the polymer inside of the bag, it will not shrink (or swell), demonstrating that the resulting hydrogel inside of the bag still has the same osmotic pressure as the polymer solution outside of the bag. This thought experiment is a corollary to the well-known c^* theorem, which states that a semi-dilute hydrogel made from flexible polymers will swell under its own osmotic pressure until it reaches c^* [17]. A consequence of this thought experiment and the c^* theorem is that the hydrogel will not compress unless the externally applied pressure is greater than the osmotic pressure of the hydrogel. This behavior holds whether the applied pressure is generated osmotically by a polymer solution, or mechanically by a steel plate or glass indenter – both types of pressure are mechanically resisted by kicks of the fluctuating polymers within the hydrogel. This type of response to applied pressure also reveals the difference between osmotic pressure and elastic modulus; in linear elasticity there is no threshold for deformation and arbitrarily small pressures can generate strain.

5. Conclusions

We have tested how the classical ideas of polymer physics and osmotic pressure manifest in the contact mechanics of hydrogels. Indentation experiments show that hydrogels respond to local contact pressures as predicted by Hertz' theory for elastic bodies, in agreement with previous studies using dead weight loads [21]. Tests are performed at relatively low pressures where Hertz' theory should apply, and find no evidence of volumetric compression of polymer or associated fluid flow. Long-time relaxations in hydrogels under local contact pressures appear to be associated with the diffusive re-structuring of the gel, driven by the gentle bias imposed by the indenter at the gel surface. Bulk compression tests confirm the classical notion that a hydrogel in equilibrium has the same osmotic pressure as a polymer solution having

the same c^*, and cannot be compressed unless the applied pressure exceeds the polymer osmotic pressure. In the future, it will be interesting to consider how the observations made here break down when conical indenters or sharp AFM tips are used to indent hydrogels. In these cases, the pressure near the apex of the indenter may exceed the polymer osmotic pressure, while the average pressure across the entire indented surfaces may remain less than the polymer osmotic pressure. It will also be valuable to test whether polymer osmotic pressure controls the contact mechanics of tissues like cartilage, where the different micro-structure of each cartilage stratum may preclude or augment the relative contribution of osmotic pressure from flexible polymers.

Acknowledgements

This work was funded by Alcon Laboratories.

References

[1] S. Van Vlierberghe, P. Dubruel, E. Schacht, Biopolymer-based hydrogels as scaffolds for tissue engineering applications: a review, Biomacromolecules 12 (2011) 1387–1408, http://dx.doi.org/10.1021/bm200083n.

[2] C.M. Kirschner, K.S. Anseth, Hydrogels in healthcare: from static to dynamic material microenvironments, Acta Mater. 61 (2013) 931–944, http://dx.doi.org/10.1016/j.actamat.2012.10.037.

[3] C.T. McKee, J.A. Last, P. Russell, C.J. Murphy, Indentation versus tensile measurements of Young's modulus for soft biological tissues, Tissue Eng. Part B. Rev. 17 (2011) 155–164, http://dx.doi.org/10.1089/ten.teb.2010.0520.

[4] M. Stolz, R. Raiteri, A.U. Daniels, M.R. VanLandingham, W. Baschong, U. Aebi, Dynamic elastic modulus of porcine articular cartilage determined at two different levels of tissue organization by indentation-type atomic force microscopy, Biophys. J. 86 (2004) 3269–3283, http://dx.doi.org/10.1016/S0006-3495(04)74375-1.

[5] R.E. Mahaffy, C.K. Shih, F.C. MacKintosh, J. Käs, Scanning probe-based frequency-dependent microrheology of polymer gels and biological cells, Phys. Rev. Lett. 85 (2000) 880–883, http://dx.doi.org/10.1103/PhysRevLett.85.880.

[6] A.A. Pitenis, J.M. Urueña, K.D. Schulze, R.M. Nixon, A.C. Dunn, B.A. Krick, W.G. Sawyer, T.E. Angelini, Polymer fluctuation lubrication in hydrogel gemini interfaces, Soft Matter 10 (2014) 8955–8962, http://dx.doi.org/10.1039/C4SM01728E.

[7] J.M. Urueña, A.A. Pitenis, R.M. Nixon, K.D. Schulze, T.E. Angelini, W. Gregory Sawyer, Mesh size control of polymer fluctuation lubrication in gemini hydrogels, Biotribology 1 (2015) 24–29, http://dx.doi.org/10.1016/j.biotri.2015.03.001.

[8] R.K. Jain, Transport of molecules in the tumor interstitium: a review, Cancer Res. 47 (1987).

[9] M.A. Swartz, M.E. Fleury, Interstitial flow and its effects in soft tissues, Annu. Rev. Biomed. Eng. 9 (2007) 229–256, http://dx.doi.org/10.1146/annurev.bioeng.9.060906.151850.

[10] H. Wang, Theory of Linear Poroelasticity with Applications to Geomechanics and Hydrogeology, Princeton University Press, Princeton NJ, 2000.

[11] Y. Hu, X. Zhao, J.J. Vlassak, Z. Suo, Using indentation to characterize the poroelasticity of gels, Appl. Phys. Lett. 96 (2010) 121904, http://dx.doi.org/10.1063/1.3370354.

[12] E.P. Chan, Y. Hu, P.M. Johnson, Z. Suo, C.M. Stafford, Spherical indentation testing of poroelastic relaxations in thin hydrogel layers, Soft Matter 8 (2012) 1492–1498, http://dx.doi.org/10.1039/C1SM06514A.

[13] Y. Hu, E.P. Chan, J.J. Vlassak, Z. Suo, Poroelastic relaxation indentation of thin layers of gels, J. Appl. Phys. 110 (2011) 86103, http://dx.doi.org/10.1063/1.3647758.

[14] A.C. Dunn, W.G. Sawyer, T.E. Angelini, Gemini interfaces in aqueous lubrication with hydrogels, Tribol. Lett. 54 (2014) 59–66, http://dx.doi.org/10.1007/s11249-014-0308-1.

[15] B.A. Krick, J.R. Vail, B.N.J. Persson, W.G. Sawyer, Optical in situ micro tribometer for analysis of real contact area for contact mechanics, adhesion, and sliding experiments, Tribol. Lett. 45 (2012) 185–194, http://dx.doi.org/10.1007/s11249-011-9870-y.

[16] A.C. Dunn, J.M. Urueña, E. Puig, V.L. Perez, W.G. Sawyer, Friction coefficient measurement of an in vivo murine cornea, Tribol. Lett. 49 (2013) 145–149, http://dx.doi.org/10.1007/s11249-012-0033-6.

[17] P.-G. De Gennes, Scaling Concepts in Polymer Physics, Cornell University Press, 1979.

[18] J.G.H. Joosten, J.L. McCarthy, P.N. Pusey, Dynamic and static light scattering by aqueous polyacrylamide gels, Macromolecules 24 (1991) 6690–6699, http://dx.doi.org/10.1021/ma00025a021.

[19] S. Mallam, F. Horkay, A.M. Hecht, E. Geissler, Scattering and swelling properties of inhomogeneous polyacrylamide gels, Macromolecules 22 (1989) 3356–3361, http://dx.doi.org/10.1021/ma00198a029.

[20] J. Klein, Hydration lubrication, Friction 1 (2013) 1–23, http://dx.doi.org/10.1007/s40544-013-0001-7.

[21] D. Lee, M.M. Rahman, Y. Zhou, S. Ryu, Three-dimensional confocal microscopy indentation method for hydrogel elasticity measurement, Langmuir 31 (2015) 9684–9693, http://dx.doi.org/10.1021/acs.langmuir.5b01267.